

Adsorption and Fluid-mixing Characteristics of Packed Bed Catalysts with Blow-by Sections

Part II. A Theoretical Approach to the Concentration Distribution

By

Tomoyuki INUI*, Masaki FUNABIKI** and Kenichi FUKUI***

(Received December 26, 1985)

Abstract

A theoretical analysis of the fluid-mixing and adsorption characteristics in packed bed catalysts with blow-by sections was conducted. A modified model of a partition gas chromatography that incorporates the effects of the blow-by section is proposed. A strong correlation between the simulated concentration-time curve predicted from this theoretical model and the experimental data was obtained.

1. Introduction

For rapid catalytic reactions, the rate determining step is dependent upon the input rate of reactants, the passage of a part of the unreacted or partially converted reactants to the distal part of the catalyst bed by way of a blow-by section which can be anticipated to produce a more uniform reaction distribution throughout the reactor. Various blow-by devices have been tested for this purpose in practical catalytic reactions¹⁾. However, quantitative studies on the adsorption and fluidmixing characteristics of a flow apparatus containing blow-by sections have been scarcely reported. Efforts have been directed toward theoretical descriptions of the concentration distribution for various types of flow apparatus²⁻³⁾. However, models incorporating blow-by sections up until now have not been theoretically analyzed with regard to their fluid-mixing characteristics.

In our previous paper¹⁾, packed tubes incorporating either semicircular or cylindrical blow-by sections were analyzed. A spherical catalyst support made of silica, having a meso-macro bimodal pore-structure and a large surface area, was

* Department of Hydrocarbon Chemistry, Faculty of Engineering, Kyoto University, Sakyo-ku, Kyoto 606.

** Present address: Nippon Engelhard Co. Ltd., Numadzu.

*** Present address: Kyoto Institute of Technology, Sakyo-ku, Kyoto 606.

used to pack the tubes. Various factors affecting the exit age-distribution function, $E(\theta)$, were examined by means of a pulse technique using either N_2 or C_2H_4 as a tracer. $E(\theta)$ was analyzed empirically by dividing the $E(\theta)$ plots into two parts, a blow-by part, B , and a residence part, R .

In this paper, for a system having such a blow-by section, we describe a theoretical approach to the concentration-time function $E(t)$ to elucidate the relationship between the structure of the apparatus and the distribution of the adsorptive tracer through the packed tube. A modified model of a partition gas chromatography that gives consideration to the blow-by part is proposed. The concentration-time curve $E(t)$ for the tracer simulated by this theoretical analysis is examined by a comparison with $E(t)$ derived from the experimental data.

2. Theory

A model of the packed flow tube containing a blow-by section is shown in Fig. 1. The packed column is divided into equivalent longitudinal sections of theoretical plates. Each theoretical plate is divided into a blow-by part and a packed part, the latter consisting of both a mobile and an immobile phase. The volume, the concentration of the adsorbate, and the flow rate through each part of each longitudinal section are represented by symbols which are shown in Fig. 1.

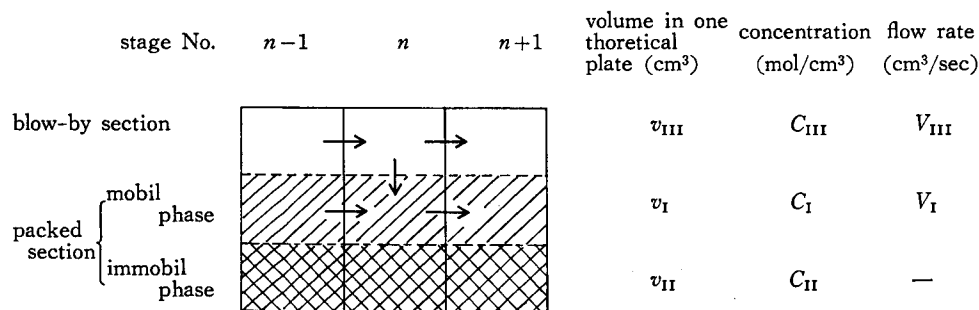


Fig. 1. Partition chromatography stages for flow tubes with blow-by section.

Moles of the adsorbate remaining in the n^{th} plate per unit time, dt (sec), can be expressed as in Eq. (1) for each packed and blow-by part, respectively, by taking into account the total volume of material passing through each theoretical plate per unit time.

$$C_{I(n-1)}V_I dt - C_{I(n)}V_I dt + k\{C_{III(n)} - C_{I(n)}\} dt = v_I dC_{I(n)} + v_{III} dC_{III(n)} \quad (1)$$

$$C_{III(n-1)}V_{III} dt - C_{III(n)}V_{III} dt - k\{C_{III(n)} - C_{I(n)}\} dt = v_{III} dC_{III(n)}$$

The term k in this equation is the mass-transfer coefficient as defined by Eq. (2):

$$k = \frac{\bar{D}y}{d} \quad (\text{cm}^2/\text{sec}) \quad (2),$$

where \bar{D} is the mean diffusion coefficient (cm²/sec), \bar{d} is the mean distance between the packed part and the blow-by part (cm), and \bar{y} is the mean distance between the blow-by part and the interphase between the mobile and immobile phases of the packed part per theoretical plate. The adsorbate is assumed to obey the adsorption equilibrium defined in Eq. (3):

$$C_{II(n)} = C_{I(n)}/K \quad (3),$$

where K is the distribution factor. Boundary conditions at time $t=0$ are:

$$\begin{aligned} C_{I(0)} &= C_{III(0)} = C_0 \\ C_{I(1)} &= C_{I(2)} = \dots = 0 \\ C_{III(1)} &= C_{III(2)} = \dots = 0 \end{aligned}$$

where C_0 is the inlet adsorbate concentration (mol/cm³). Eq. (4) is obtained by rearranging Eq. (1):

$$\begin{aligned} v_E \frac{dC_{I(n)}}{dt} &= V_I \{C_{I(n-1)} - C_{I(n)}\} + k \{C_{III(n)} - C_{I(n)}\} \\ v_{III} \frac{dC_{III(n)}}{dt} &= V_{III} \{C_{III(n-1)} - C_{III(n)}\} - k \{C_{III(n)} - C_{I(n)}\} \end{aligned} \quad (4),$$

where v_E is the volume of one effective plate (cm³), as defined by Eq. (5)⁴:

$$v_E = v_I + \frac{v_{II}}{K} \quad (5).$$

By substituting, $\frac{C_{I(n)}}{C_0} = x_n$, $\frac{C_{III(n)}}{C_0} = y_n$, $\frac{v_E}{V_I} = \kappa$, $\frac{v_{III}}{V_{III}} = \lambda$, $\frac{k}{V_I} = a$, and $\frac{k}{V_{III}} = b$, Eq. (4) can be transformed into the fundamental Eq. (6):

$$\begin{aligned} \left(\kappa \frac{d}{dt} + 1 + a\right)x_n &= x_{n-1} + ay_n \\ \left(\lambda \frac{d}{dt} + 1 + b\right)y_n &= y_{n-1} + bx_n \end{aligned} \quad (6),$$

where

$$\begin{aligned} n &= 1, 2, \dots, \infty; \text{ and at } t=0 \\ x_0 &= 1, \quad x_1 = x_2 = \dots = x_n = 0 \\ y_0 &= 1, \text{ and } y_1 = y_2 = \dots = y_n = 0 \end{aligned}$$

When there is little interaction between the packed and blow-by parts, such that a and b are much less than 1, then Eq. (6) becomes Eq. (7) by neglecting the terms having coefficients a and b :

$$\begin{aligned} \left(\kappa \frac{d}{dt} + 1\right)x_n &= x_{n-1} \\ \left(\lambda \frac{d}{dt} + 1\right)y_n &= y_{n-1} \end{aligned} \quad (7).$$

The approximate solution of Eq. (7) is given in Eq. (8):

$$x_n = \frac{(t/\kappa)^n e^{-\frac{1+a}{\kappa}t}}{n!} \quad (8).$$

$$y_n = \frac{(t/\lambda)^n e^{-\frac{1+b}{\lambda}t}}{n!}$$

If M_n (mol/sec) is the moles per second of the adsorbate eluted from the n th plate, then M_n can be expressed as Eq. (9):

$$\begin{aligned} M_n &= C_{I(n)} V_I + C_{III(n)} V_{III} \\ &= \frac{C_0}{n!} \left\{ V_I \left(\frac{V_I}{v_E} t \right)^n e^{-\frac{V_I+k}{v_E} t} + v_{III} \left(\frac{V_{III}}{v_{III}} t \right)^n e^{-\frac{V_{III}+k}{v_{III}} t} \right\} \end{aligned} \quad (9).$$

Accordingly, the total amount of eluted adsorbate can be determined from Eq. (10):

$$\int_0^\infty M_n dt = C_0 \left\{ v_E \left(\frac{V_I}{V_I+k} \right)^{n+1} + v_{III} \left(\frac{V_{III}}{V_{III}+k} \right)^{n+1} \right\} \quad (10).$$

In order to compare the simulated values with experimental data, the following transformation was made. The curve $E(t)$ vs. t was obtained by normalizing the experimental curve¹³ according to Eq. (11):

$$\int_0^\infty E(t) dt = 1 \quad (11).$$

If Eq. (10) is normalized to a volume of 1, then $M_n(t)$ can be equated to $E(t)$ by Eq. (12):

$$\begin{aligned} M_n(t) = E(t) &= \frac{M_n}{\int_0^\infty M_n dt} \\ &= \frac{1}{n!} \cdot \frac{V_I \left(\frac{V_I}{v_E} t \right)^n e^{-\frac{V_I+k}{v_E} t} + v_{III} \left(\frac{V_{III}}{v_{III}} t \right)^n e^{-\frac{V_{III}+k}{v_{III}} t}}{v_E \left(\frac{V_I}{V_I+k} \right)^{n+1} + v_{III} \left(\frac{V_{III}}{V_{III}+k} \right)^{n+1}} \end{aligned} \quad (12),$$

where,

$$\int_0^\infty M_n(t) dt = \int_0^\infty E(t) dt = 1 \quad (13).$$

Since the mean residence time τ is expressed by Eq. (14):

$$\begin{aligned} \tau &= \frac{\int_0^\infty t M_n dt}{\int_0^\infty M_n dt} \\ &= \frac{(n+1) \frac{v_E}{V_I+k} v_E \left(\frac{V_I}{V_I+k} \right)^{n+1} + \frac{v_{III}}{V_{III}+k} v_{III} \left(\frac{V_{III}}{V_{III}+k} \right)^{n+1}}{v_E \left(\frac{V_I}{V_I+k} \right)^{n+1} + v_{III} \left(\frac{V_{III}}{V_{III}+k} \right)^{n+1}} \end{aligned} \quad (14),$$

then Eq. (15) is obtained as the approximate equation,

$$\tau \doteq \frac{(n+1)}{2} \left(\frac{v_E}{V_I+k} + \frac{V_{III}}{V_{III}+k} \right) \quad (15).$$

Further, since the maximum value of $M_n(t)$ is given as Eq. (16):

$$\begin{aligned} \frac{dM_n}{dt} &= \frac{C_0}{n!} \left\{ V_I \left(\frac{V_I}{v_E} t \right)^n e^{-\frac{V_I+k}{v_E} t} \cdot t^{n-1} \left(n - \frac{V_I+k}{v_E} t \right) \right. \\ &\quad \left. + v_{III} \left(\frac{V_{III}}{v_{III}} t \right)^n \cdot t^{n-1} e^{-\frac{V_{III}+k}{v_{III}} t} \left(n - \frac{V_{III}+k}{v_{III}} t \right) \right\} \end{aligned} \quad (16),$$

the time t_{\max} at which $M_n(t)$ attains the maximum can be expressed approximately by Eq. (17):

$$t_{\max} = \frac{n}{2} \left(\frac{v_{\mathcal{F}}}{V_{\text{I}} + k} + \frac{v_{\mathcal{F}}}{V_{\text{III}} + k} \right) \quad (17).$$

Both Eqs. (15) and (17) may be useful for evaluating the value of k .

3. Results and Discussion

Data obtained using 10.7 mm inner diameter by 50 cm long tubes that had 44.8 cm³ total packing volumes, as reported in Part I of this paper¹⁾, are used below to test the validity of the above theoretical derivations.

3.1. Determination of Parameters

3.1.1. v_{I} , v_{II} , and v_{III}

The values of v_{I} , v_{II} , and v_{III} for the fully packed, the various semicircular blow-by packed, vacant, and cylindrical blow-by packed tubes are listed in Table 1. The sectional areas for the blow-by sections were identical to those employed in the 13/16 semicircular blow-by packed tubes.

Table 1. Volume values in each theoretical plate for various blow-by packings.

packing ratio	v_{I}/n cm ³	v_{II}/n cm ³	v_{III}/n cm ³
1	21.3	23.5	0
15/16	20.0	22.1	2.7
14/16	18.6	20.6	5.6
13/16	17.3	19.3	8.2
12/16	16.0	17.7	11.1
8/16	10.6	11.8	22.4
4/16	5.4	6.0	33.4
0	0	0	44.8
cylindrical blow-by packing	18.0	19.9	6.2

3.1.2. $v_{\mathcal{F}}$

Since contribution by blow-by sections could be neglected, Eq. (12) for fully packed tubes was calculated by setting $k=0$, and $V_{\text{III}}=0$. However, for tubes with blow-by sections, $v_{\mathcal{F}}$ was obtained from Eq. (15) by setting $K=0.096$, which is the value obtained for K when the experimentally determined values are substituted into Eq. (12).

3.1.3. V_{I} and V_{III}

If $V(\text{cm}^3/\text{sec})$ is the total flow rate, then V_{I} and V_{III} are calculated by Eq. (18):

Table 2. Flow rate values in each theoretical plate for various blow-by packings.

packing ratio	V	V _I	V _{III}
1	12.3	12.3	
15/16	12.5	11.0	1.46
14/16	12.3	9.45	2.85
13/16	13.1	8.86	4.24
12/16	12.2	7.18	5.02
8/16	12.5	4.02	8.48
4/16	12.6	1.75	10.9
cylindrical blow-by packing	12.6	9.38	3.22

$$\frac{v_I}{V_I} = \frac{v_{III}}{V_{III}} = \frac{(v_I + v_{III})}{V} \quad (18).$$

Seven hundred and fifty cm³/min was adopted as the value of V that was obtained from the data presented in the first report¹⁾. Those results are listed in Table 2.

3.1.4. k

k was calculated from Eq. (2). The mean diffusion coefficient for the C₂H₄-H₂ binary system at 20°C, 0.540 cm²/sec, was used as \bar{D} . The value of \bar{d} was determined as the distance between the centers of gravity for the surfaces of the packed and blow-by sections. These values are listed in Table 3.

Table 3. The calculated values for the mass-transfer coefficient in each theoretical plate for various blow-by packings.

packing ratio	\bar{d}/n	\bar{y}/n	k/n
1	0	0	0
15/16	0.485	33.5	37.3
14/16	0.470	41.4	47.5
13/16	0.453	45.8	54.6
12/16	0.445	48.8	59.2
8/16	0.436	53.4	66.2
4/16	0.445	48.8	59.2
cylindrical blow-by packing	0.398	55.6	75.4

3.2. Simulation Results

When flow rates were varied within a range of 20~1300 cm³/min, differences in the E(t) curves for a flow rate of 500 cm³/min were rather large due to the flow through the blow-by. Increasing the flow rate above 500 cm³/min, however, did not produce significant changes in the E(t) curves for flow tubes incorporating blow-by sections¹⁾. Therefore, in the present study a flow rate of 750 cm³/min was adopted.

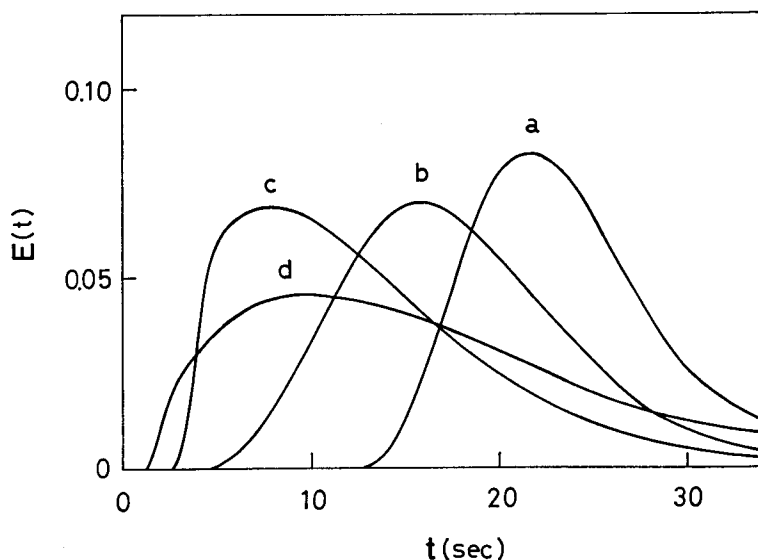


Fig. 2. $E(t)$ - t curves for various packing ratios. a, full packing; b, cylindrical blow-by packing; c, semicircular blow-by packing, 8/16 ratio; d, semicircular blow-by packing, 13/16 ratio.

$E(t)$ - t curves for various flow tube packing ratios are shown in Fig. 2. Integral numbers for the values of H , the height equivalent to a theoretical plate, calculated from observed data¹⁾ were substituted for n in Eq. (12). Eq. (12) was calculated for consecutive integral values of t between 1 and 40 sec., using a Texas Instruments Model SR-56 programmable calculator. When the values of k listed in Table 3 were used in Eq. (12), the simulated $E(t)$ - t curves did not fit with the observed $E(t)$ - t curves. However, when the values of k calculated from Eq. (15) or (17) after substituting the observed values for τ or t_{\max} were used, good agreement between the

Table 4. Summary of the values of n and k used in the simulation calculations and correspondence of simulated $E(t)$ - t curve with observed $E(t)$ - t curves.

packing ratio	n calculated by H	n adopted	k calculated	k adopted	$\frac{k \text{ adopt.}}{k \text{ calc.}}$	correspondence
1	20.7	21	0	0	—	vary good
15/16	5.9	7	5.33	2.67	0.50	almost agree
14/16	1.4	2	23.8	8.91	0.38	fairly good
13/16	0.6	2	27.3	11.5	0.42	good
12/16	0.6	2	29.6	12.0	0.41	fairly discrete
8/16	0.9	2	33.1	16.6	0.50	no agreement
4/16	3.3	3	19.8			no agreement
cylindrical	8.1	8	9.43	4.72	0.50	very good

simulated and observed $E(t)-t$ curves was obtained for a higher packing ratio as shown in Table 4 and Figs. 3, 4, and 6. The simulated curves agree well with the observed curves for packing ratios between the full packed bed and the 13/16 packed bed in

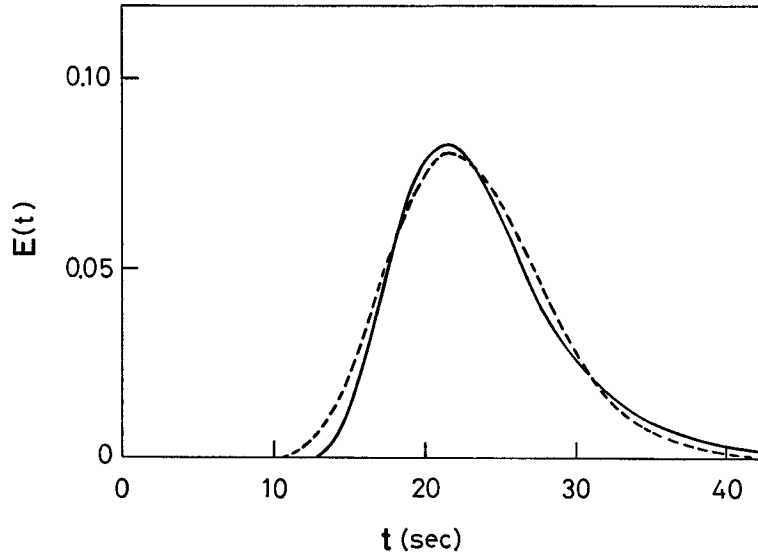


Fig. 3. Comparison of simulated and experimental $E(t)-t$ curves for fully packed flow tube. Solid line, experimental curve; dotted line, simulated curve.

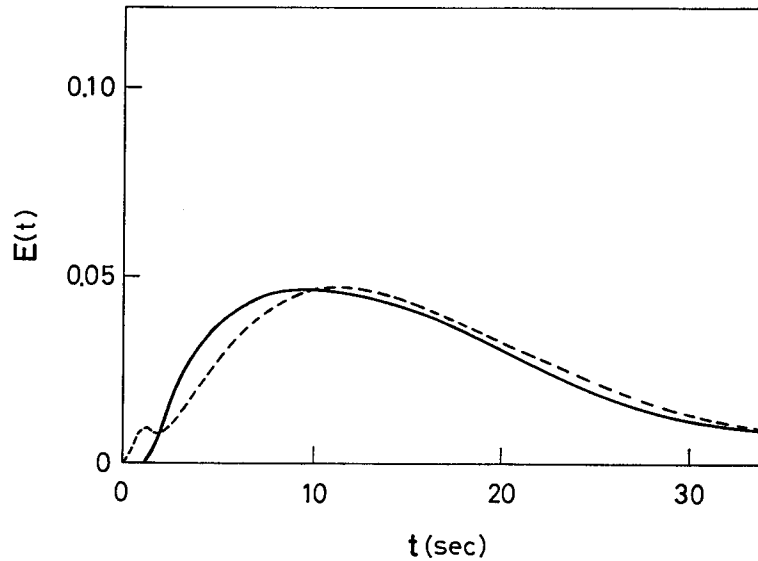


Fig. 4. Comparison of simulated and experimental $E(t)-t$ curves for the 13/16 semicircular blow-by packing. Solid line, experimental curve; dotted line, simulated curve.

which the flow contribution at the blow-by section was maximum and especially, for the cylindrical blow-by packing. However, as shown in Fig.5, when the packing ratio was smaller than 12/16, discrepancies between the simulated and observed

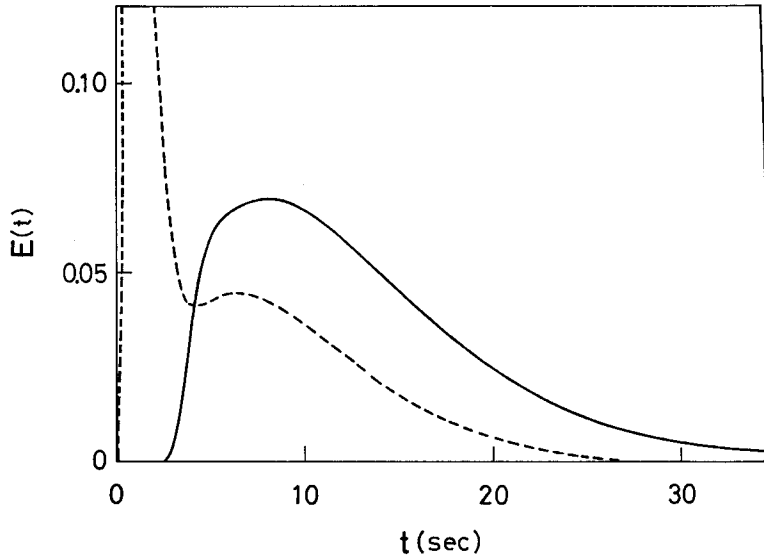


Fig. 5. Comparison of simulated and experimental $E(t)$ - t curves for the 8/16 semicircular blow-by packing. Solid line, experimental curve; dotted line, simulated curve.

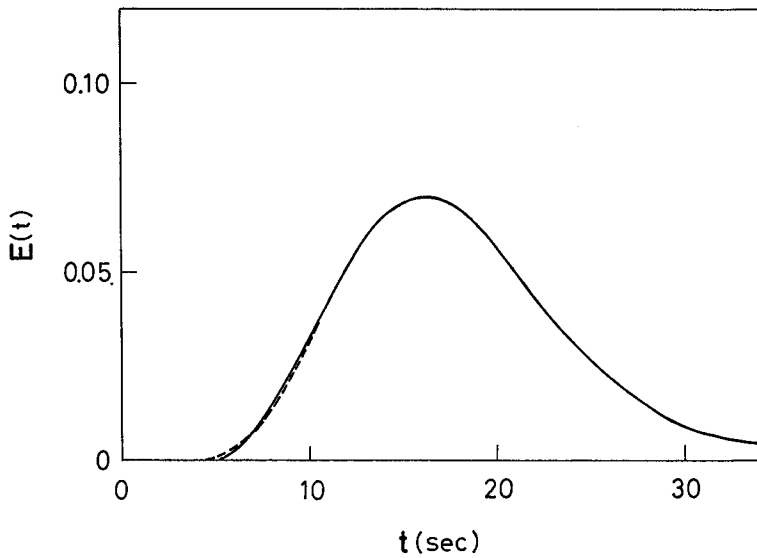


Fig. 6. Comparison of simulated and experimental $E(t)$ - t curves for the cylindrical blow-by packing. Solid line, experimental curve; dotted line, simulated curve.

curves became greater due to decreased contributions of the blow-by section to the total flow through the packed tube, which is reflected as increases in the blow-by term of Eq. (12).

In conclusion, when one determines the values of k from the data obtained with a fully packed bed and n from the observed H , the values of $E(t)$ predicted from Eq. (12) provide satisfactory estimates for the useful range of blow-by packings as concluded in the previous paper¹⁾, when the k values are multiplied by a constant factor of 0.4~0.5 (Table 4). Thus, the model and equations proposed here can be considered to be effective for analysis and estimation of the contribution of blow-by sections in packed-bed systems.

References

- 1) Inui, T., Funabiki, M. and Shingu, H., *Memoirs Fac. Eng. Kyoto Univ.* **48**, No.2, 49 (1986).
- 2) Levenspiel, O., "Chemical Reaction Engineering", 1962, John Wiley & Sons, INC., New York, p.242.
- 3) Himmelblau, D.M. and Bischoff, K.B., "Process Analysis and Simulation Deterministic Systems", 1967, John Wiley & Sons. INC., New York, p.59.
- 4) Van Deemter, J.J., Zuiderweg, F.J. and Klinkenberg, A., *Chem. Eng. Sci.*, **5**, 271 (1956).